Heliyon 6 (2020) e04621

Contents lists available at ScienceDirect

Heliyon

journal homepage: www.cell.com/heliyon

Research article

A kinetic study and mechanisms of reduction of *N, N′*-phenylene*bis*(salicyalideneiminato)cobalt(III) by L-ascorbic acid in DMSO-water medium

S. Abdulsalam [a,*], S.O. Idris [a], G.A. Shallangwa [a], A.D. Onu [b]

[a] *Department of Chemistry, Ahmadu Bello University, Zaria, Nigeria*
[b] *Department of Chemistry, Federal College of Education, Zaria, Nigeria*

ARTICLE INFO

Keywords:
Inorganic chemistry
Physical chemistry
Kinetics
Mechanism
L-ascorbic acid
Outer-sphere mechanism
Mixed aqueous medium

ABSTRACT

The kinetics of reduction of *N, N′*-phenylene*bis*-(salicylideneiminato)cobalt (III), referred to as $[Co(Salophen)]^+$ by L-ascorbic acid (H_2A) was studied in mixed aqueous medium (DMSO:H_2O; 1:4 v/v) under pseudo-first-order conditions at 33 ± 1 °C, μ = 0.1 mol dm^{-3} (NaCl) and λ_{max} = 470 nm. L-ascorbic acid was oxidized to dehydroascorbic acid with kinetics that was first order in both the $[H_2A]$ and $[Co(Salophen)^+]$ and second-order overall. The reaction involves two parallel reaction pathways; an acid-dependent and the inverse acid-dependent pathways. The inverse acid pathway shows that there is a pre-equilibrium step before the rate determining-step in which a proton is lost. The kinetics followed negative Brønsted–Debye salt effect. Evidence was obtained for the presence of free radicals but none to support the formation of an intermediate complex of significant stability during the reaction. Overall, the data obtained suggest an outer-sphere mechanism for the reaction. A plausible mechanism is proposed.

1. Introduction

With the improvement of Cis-platin in recent years, the investigation of the complexes of metal as compounds of anticancer has produces favorable outcomes in the field of medicinal inorganic chemistry (Lippert, 1999). The utilization of different inorganic complexes and other organometallic compounds to treat different kind of ailments have been comprehensively researched (Failes et al., 2007; Lippert, 1999). Literature review revealed that metal complexes are tumor compound delivery agents, and some environmental factors (pH, light and redox process) can trigger their activation (Graf and Lippard, 2012; Mari et al., 2015; Pizarro et al., 2010; Renfrew, 2014; Yamamoto et al., 2012). Transition metal complexes can increase the activity of cytochrome P450, an important class of enzymes that catalyzes a wide variety of reactions such as oxygen transfer to heteroatoms, epoxidation of olefins, hydroxylation of aromatic hydrocarbons and oxidation degradation of xenobiotics (Salavati-niasari, 2006).

Recent investigations revealed that metal complexes such as Pt^{IV}, Ru^{III}, and Co^{III} (Bonnitcha et al., 2012; Graf and Lippard, 2012) produced in large quantity has been reported to bio-reductively target solid tumor-cancer in hypoxia environments (Blazevic et al., 2017; Webb and Walsby, 2013). The inability of Co^{II} and other pro compounds to bio-reductive tune reduction potential beyond lower end of range (-420 to -150mV) to pave way for the selective activation in solid-tumor hypoxic environment (Denny, 2010; Failes et al., 2007; Kizaka-Kondoh et al., 2003; Renfrew et al., 2013; Ware et al., 1997). Some researchers previously proposed and investigated the probability of tuning reduction potential of metal complexes beyond large lower range (-420 to -150mV) through structural alteration at ring para-position (Chiang et al., 2014, 2012; Clarke and Storr, 2016; Zhang et al., 2017). Their research lead to the metal complexes of octahedral Co^{III} salen series. Moreover, some group of investigators also proposed bi-reduction to Co^{II} and ligand rearrangement and exchange respectively would dynamically free pathway for axial location of cytotoxic ligands(Gust et al., 2004; Kianfar and Khavasi, 2016).

Various metal complexes of salophen (*bis*(salicylidene)phenylenediamine) type ligands find applications in the intercalation of DNA base pairs and also used for potentiometric discoveries of basic anions existing in biological and environmental systems (Yilmaz et al., 2017). Furthermore, Co(II)Salophen complexes were used for oxidation of water under visible light irradiation, with *tris*(bipyridine)ruthenium (III) as the

* Corresponding author.
E-mail address: write2mesafiyya@yahoo.com (S. Abdulsalam).

https://doi.org/10.1016/j.heliyon.2020.e04621
Received 6 March 2020; Received in revised form 17 March 2020; Accepted 30 July 2020

photosensitizer and persulphate as the sacrificial electron acceptor (Pizzolato et al., 2013).

L-ascorbic acid (H_2A) is well known for its reducing properties in aqueous solutions. It can be oxidized by one electron to a radical state or doubly oxidized to the stable form called dehydroascorbic acid. H_2A is special owing to the stability of its radical ion called "semidehydro-ascorbate", dehydro-ascorbate. However, being a good electron donor, excess ascorbate in the presence of free metal ions cannot only promote but also initiate free radical reactions (Jattinagoudar et al., 2013). H_2A has also been well-established as an antioxidant and a reliable redox reagent and has attracted great interest from many scientists in the field of life and physical sciences. This multifunction of H_2A aroused series of investigations on transition metal complexes oxidation, particularly trivalent state (Salem and Gemeay, 1996). A compendium of the reactions of H_2A has been published by Davies (1992). But in recent years, the mode of action (mechanism) of physiological function (activities) has becomes topic of discussion (Alioke et al., 2012). In order to understand the mode of action of H_2A complex, the kinetics of reduction of $[CoSalophen]^+$, (Salophen = Bis(Sali-cylidene)phenylenediamine) with H_2A was comprehensively carried out.

So far, various kinetics and mechanisms of Salophen complexes of iron (Ibrahim et al., 2019a, 2019b; Subramaniam et al., 2014), cobalt (Abdulsalam et al., 2020) and manganese (Jena et al., 2018) have been recently reported. Herein, we report on the kinetic study and mechanisms of reduction of *N, N′*-phenylene*bis* (salicyalideneiminato)cobalt (III) complex ($[Co(Salophen)]^+$) by H_2A in a mixed aqueous medium.

2. Materials and method

All the chemicals used for this study were of analytical grade and were used without further purification. The rates of reactions were studied by monitoring the reaction mixture as the absorbance decreases with increasing reaction time at 470 nm on a SHERWOOD colorimeter 254. L-ascorbic (BDH) and sodium chloride salt (M&B) were used as a reducing agent and to stabilize the strength of ions in the reaction medium respectively. Also, 50 cm^3 of DMSO was used to prepare DMSO-H_2O solution of ratio 1:4 (v/v). Cobalt (II) chloride hexahydrate, salicyaldehyde, 1,2-phenylenediamine, chloroform, ethanol, H_2O_2, and diethyl ether were all obtained from Merck. The Schiff base, *Bis*(salicylidene)-1,2-phenylenediamine, (Salophen) and the complex, *N,N′*-phenylene*bis*-(salicylideneiminato)cobalt (III), ($[Co(Salophen)]^+$) were synthesized and characterized according to earlier published report (Pizzolato et al., 2013; Abdulsalam et al., 2020). The complex structure is revealed in Scheme 1 below.

The molar conductivity of [Co(Salophen)]Cl in H_2O: DMSO is reliable to 1:1 electrolytic ratio. The occurrence of $[Fe(Salphen)]^+$ in DMSO-H_2O (ratio 1:4 v/v), $[Fe\ (salen)]^+$ species in DMSO–H_2O (ratio 4:1 v/v), CH_3CN–H_2O in (ratio 1:1 v/v) and [Co(Salophen).H_2O] in (H_2O) solvent systems have been reported previously (Ibrahim et al., 2019a; Liou and Wang, 2000; Pizzolato et al., 2013; Subramaniam et al., 2014).

2.1. Kinetic measurement

Using the 254 SHERWOOD colorimeter model, the rate of reaction was calculated by observing a reduction in absorbance of $[Co(Salophen)]^+$ at 470 nm. The concentration of $Co(Salophen)^+$ was maintained at 3×10^{-4} mol dm^{-3}. With $[H_2A]$ of minimum 10-fold excess over $[Co(Salophen)^+]$ at 0.1 mol dm^{-3} of NaCl and 2.0×10^{-3} mol dm^{-3} of $[H^+]$ (HCl), kinetics investigations were followed under pseudo first order conditions. The Graphs of log (At − A∞) against time were made (where A∞ and At are the absorbance at the end of the reaction and at time t, respectively), and pseudo-first-order rate constants (k_1), were determined from the slopes of the graphs. The second-order rate constants (k_2), were gotten from Eq. (1).

$$k_2 = k_1/[H_2A] \quad (1)$$

Using HCl, the hydrogen ion concentration's effect on the reaction rate was studied by changing the $[H^+]$ between $(1.0–9.0) \times 10^{-3}$ mol dm^{-3}, while both $[Co(Salophen)^+]$ and $[H_2A]$ were kept constant at 3.0×10^{-4} mol dm^{-3} and 12.0×10^{-3} mol dm^{-3} respectively, at $T = 33 \pm 1$ °C and $\mu = 0.1$ mol dm^{-3} (Idris et al., 2015). Moreover, keeping the concentration of the reactants constant at 33 ± 1 °C, the effect of changing the ionic strength of the reaction on the rate was examined between 0.04–0.18 mol dm^{-3}. Also, for $[X] = 3.0–18.0 \times 10^{-3}$ mol dm^{-3}, the effect of adding cation or anion ($[X] = Mg^{2+}$ or SO_4^{2-}) on the rate of reaction was studied at a fixed ionic strength, $[Co(Salophen)^+]$ and $[H_2A]$.

2.2. Stoichiometry, reaction products, and reaction monitoring

The stoichiometry of the reaction was control by spectrophotometric titration utilizing the mole ratio technique. The stoichiometry was assessed from a graph of absorbance against the mole ratio (Onu et al., 2009).

The H_2A oxidation product was determined quantitatively after treating the reaction blend with pyrrole, in excess trichloroacetic acid (Abiti et al., 2018). The reduction product of the cobalt (III) was observed by the addition of a few drops of potassium thiocyanate in excess acetone to the reaction product (Osunlaja et al., 2013). Under the laboratory condition, the complex $[Co(Salophen)]^+$ spectrum shows a significant maximum at 470nm. The reaction can be monitored quantitatively since product and reactant was not absorb at this region apart from the H_2A-complex.

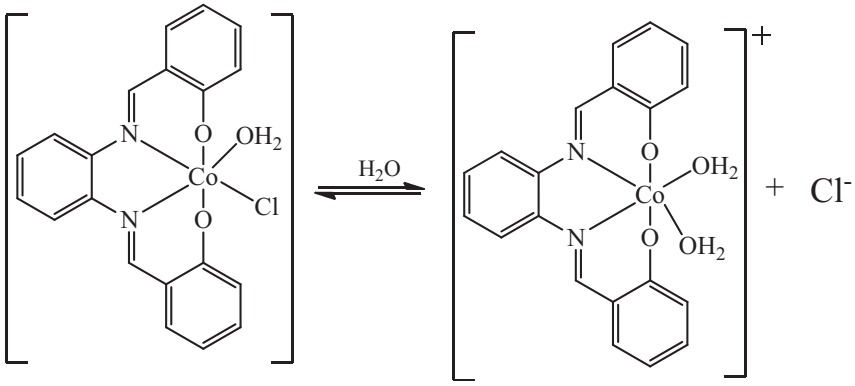

Scheme 1. Structure of the complex.

2.3. Spectroscopic, free radical study and activation parameters analysis

The complex spectrum, over a wavelength range of 400–700 nm, was compared with that of the reaction mixture, to see whether there is a shift in the wavelength of maximum absorption (λ_{max}). A Michaelis–Menten plot of $1/[H_2A]$ against $1/k_1$ for the reaction, was examined. Free radical was also investigated by adding acrylamide, after that excess methanol to a partially reacted mixtures of $[Co(Salophen)^+]$ and $[H_2A]$ (Ibrahim et al., 2019b). Using the temperature of 306 K–333 K, the effect of temperature on the reaction rate was investigated, by subjecting the temperature dependence data to analyses with the aid of an Eyring graph of 1/T against ln (k_2/T) (Eq. (2)), at constant $[H_2A]$, $[Co(Salophen)^+]$ and ionic strength. Thermodynamic parameters were also examined.

$$\ln\left(\frac{k_2}{T}\right) = \ln\left(\frac{k_B}{h}\right) + \frac{\Delta S^{\ddagger}}{R} - \frac{\Delta H^{\ddagger}}{R}\left(\frac{1}{T}\right) \quad (2)$$

3. Results and discussion

3.1. Oxidation state for cobalt outcome analysis

Cobalt (II), the reduction product of Cobalt (III) is confirmed as follows; at the completion of the reaction, potassium thiocyanate was added and a blue solution was formed due to the formation of $[Co(SCN)_4]^{2-}$. This shows that the Co(III) in the complex has been reduced to Co(II) by the H_2A. However, to obtain the equation of balanced stoichiometry, it is important to know the oxidation state of cobalt after reaction with the reductant.

3.2. The reductant product and the stoichiometry

After mixing the reaction mixture with pyrrole in excess trichloroacetic acid, blue–green color was noticed, this confirms the ascorbic acid's reductant product to be dehydroascorbic acid. The mole ratio of the reaction was found to be 2:3 (Figure 1) and can be represented by Eq. (3):

$$2[Co(Salophen)]^+ + 3H_2A + O_2 \rightarrow 2[Co(Salophen)] + 3A + 2H^+ + 2H_2O \quad (3)$$

where A is dehydroascorbic acid.

A stoichiometry of 1:1 was reported in the reduction of [Fe(Saloph)$_2$-μ-dicarpy] with ascorbic acid (Ukoha et al., 2018), and oxidation of l-ascorbic acid by pentaamminecobalt (III) ion (Dixon et al., 1995). Also, a stoichiometry of 2:1 was reported in the oxidation of ascorbic acid by hexacyanoferrate (III) (Jattinagoudar et al., 2013) and reduction of ethylenediamine tetraacetatocobaltate (III) ion by l-ascorbic acid (Abiti et al., 2018).

3.3. Kinetic analysis

In the kinetic analysis, a graph of log ($A_t - A_\infty$) against time, gave a straight line, implying that the reaction is first-order with respect to $[Co(Salophen)^+]$ (Figure 2). The order of the reaction with respect to $[H_2A]$ was determined when log k_1 was plotted against log $[H_2A]$. The slope was calculated to be 0.99 (Figure 3). For the different values of $[H_2A]$, the second-order rate constant (k_2) was fairly the same (Table 1). With respect to the reactants, the reaction shows 2nd order total, and can be signified by Eq. (4):

$$-d[Co(Salophen)^+]/dt = k_2\,[Co(Salophen)^+]\,[H_2A] \quad (4)$$

where $k_2 = (2.42 \pm 0.07)\ dm^3mol^{-1}s^{-1}$

Similar second-order overall was previously reported in the reactions of H_2A by *N, N^1*- salicylideneiminato iron (III) (Alioke et al., 2012), hexacyanoferrate (III) (Jattinagoudar et al., 2013) and *N, N^1*- ethylene*bis* (salicylideneiminato) Mn(III) (Salem and Gemeay, 1996), respectively. A fractional-order has also been reported in the reduction of [Fe(Saloph) 2-μ-dicarpy] by H_2A (Ukoha et al., 2018).

The rate of the reaction was found to decrease with an increase in $[H^+]$ (Table 1). Graph of k_2 against $[1/H^+]$ gave a positive intercept (Figure 4). This observation suggests that two parallel reaction pathways are involved in the reaction; an acid-dependent and inverse acid-dependent pathway. The inverse acid pathway shows that there was a pre-equilibrium step before the rate determining-step in which a proton is lost i.e. both the protonated and the deprotonated form of the reductant (H_2A and HA^-) are reactive at the rate-determining step (Gupta and Gupta, 1984).

Acid dependence effect of this kind is represented by Eq. (5)

$$k_H^+ = a + b\,[H^+]^{-1} \quad (5)$$

where 'a' = 0.82 $dm^3mol^{-1}\ s^{-1}$ and 'b' = $3.10 \times 10^{-3}\ s^{-1}$.

The final rate scheme for the reaction is presented in Eq. (6)

$$\frac{-d[Co(Salophen)^+]}{dt} = \left(a + b[H^+]^{-1}\right)[Co(Salophen)^+][H_2A] \quad (6)$$

Similar acid independent pathway has been reported in the reaction of H_2A by [Fe(Saloph)2-μ-dicarpy] complex (Ukoha et al., 2018) and Ru(III) ion (Khan and Shukla, 1988) respectively.

The result in Table 1 revealed that differences in the ionic strength of the reaction medium reduce the rate of reaction. A Graph of log k_2 versus $\sqrt{\mu}$ gave a slope of -1.1 (Figure 5), suggesting a negative Brønsted–Debye salt effect. This infers that the reaction proceeds via an interaction

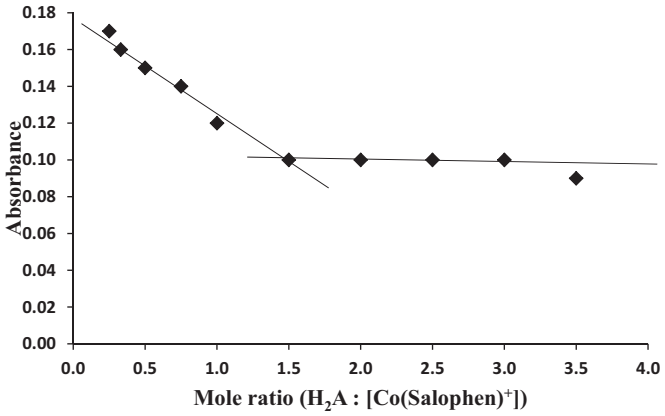

Figure 1. Plot of Absorbance against mole ratio for the reaction of $[Co(Salophen)]^+$ and H_2A at $[Co(Salophen)^+] = 3.0 \times 10^{-4}$ mol dm^{-3}, $[H_2A] = (0.5–7.0) \times 10^{-4}$ mol dm^{-3}, $[H^+] = 2.0 \times 10^{-3}$ mol dm^{-3}, μ = 0.1 mol dm^{-3}, T = 33 ± 1 °C and λ_{max} = 470 nm.

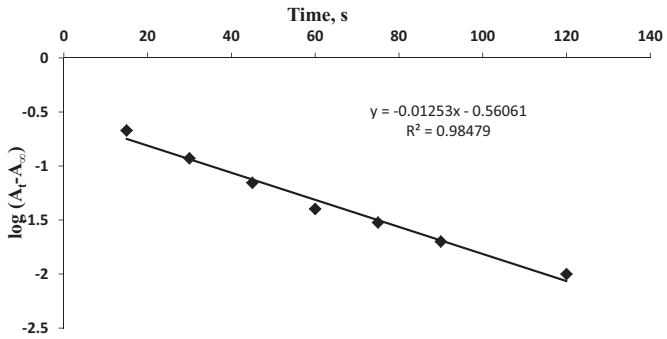

Figure 2. Typical pseudo-first order plot for the reaction of $[Co(Salophen)]^+$ and H_2A at $[Co(Salophen)^+] = 3.0 \times 10^{-4}$ mol dm^{-3}, $H_2A = 12.0 \times 10^{-3}$ mol dm^{-3}, $[H^+] = 2.0 \times 10^{-3}$ mol dm^{-3}, μ = 0.1 mol dm^{-3}, T = 33 ± 1 °C and λ_{max} = 470 nm.

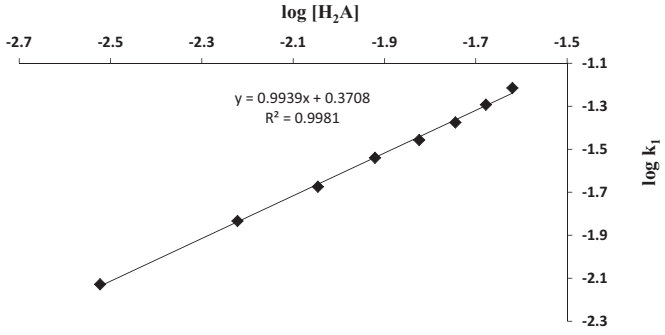

Figure 3. Plot of $\log k_1$ against log $[H_2A]$ for the reaction of $[Co(Salophen)]^+$ and H_2A at $[Co(Salophen)^+] = 3.0 \times 10^{-4}$ mol dm^{-3}, $[H^+] = 2.0 \times 10^{-3}$ mol dm^{-3}, $\mu = 0.1$ mol dm^{-3}, T = 33 ± 1 °C and $\lambda_{max} = 470$ nm.

between oppositely charged species $(Co(Salophen)^+$ & $HA^-)$ at the rate-determining step (Onu et al., 2009).

Also, added ion (SO_4^{2-} or Mg^{2+}) into the reaction mixture was found to increase the rate of reaction (Table 2). Ion catalysis is consistent with the reaction occurring without bridging ligand participation, evidence in support of the outer-sphere pathway of electron transfer (Ibrahim et al., 2019a).

3.4. Spectroscopic analysis

When the spectrum of $[Co(Salophen)^+]$ was compared with that of the reaction mixture, no shift in the λ_{max} (470nm) was observed (Figure 6). This suggests that the participation of an intermediate complex as the reaction is progressing is unlikely, evidence in support of an outer-sphere mechanism (Ibrahim et al., 2019b). The linear slope without an intercept observed in the Michaelis-Menten plot further confirmed the absence of an intermediate complex with significant stability during the reaction (Figure 7) (Onu et al., 2009).

3.5. Free radical and activation parameters analysis

A gelatinous precipitate was observed when radical scavenger (acrylamide) was added to a partially reacting mixture then excess CH_3OH, confirming the presence of free radicals in the reaction. The result of temperature dependence on rate constant is shown in Table 3. The values of activation parameters obtained from this research ($\Delta H^* = +47.70$ kJ mol^{-1}, $\Delta S^* = -82.87$ J mol^{-1} K^{-1}) favor the electron transfer process. The large negative value of entropy of activation (ΔS^*) indicates a more ordered transition state (Dixon et al., 1995).

3.6. Mechanism

Reaction schemes in Eqs. (7), (8), (9), and (10) was proposed base on the results obtained from this research.

$$H_2A \overset{K}{\rightleftharpoons} H^+ + HA^- \tag{7}$$

$$[Co(Salophen)]^+ + HA^- \underset{slow}{\overset{k_3}{\longrightarrow}} [Co(Salophen)] + HA^{\cdot} \tag{8}$$

$$[Co(Salophen)]^+ + H_2A \underset{slow}{\overset{k_4}{\longrightarrow}} [Co(Salophen)] + HA^{\cdot} + H^+ \tag{9}$$

$$H_2A + 2HA^{\cdot} + O_2 \underset{fast}{\overset{k_5}{\longrightarrow}} 3A + 2H_2O \tag{10}$$

$$Rate = k_3[Co(Salophen)^+][HA^-] + k_4[Co(Salophen)^+][H_2A] \tag{11}$$

From Equation (1)

$$[HA^-] = K\frac{[H_2A]}{[H^+]} \tag{12}$$

Substitute Equation (12) in Equation (11)

Table 1. Pseudo 1st order and 2nd order rate constants for the reaction of $[Co(Salophen)]^+$ and H_2A reaction at $[Co(Salophen)^+] = 3.0 \times 10^{-4}$ mol dm^{-3}, T = 33 ± 1 °C and $\lambda_{max} = 470$nm.

10^3 $[H_2A]$ (mol dm^{-3})	10^3 $[H^+]$ (mol dm^{-3})	μ (mol dm^{-3})	10^3k_1 (s^{-1})	k_2 (dm^3 mol^{-1} s^{-1})
3.00	2.00	0.10	7.44	2.48
6.00	2.00	0.10	14.66	2.44
9.00	2.00	0.10	21.18	2.35
12.00	2.00	0.10	28.86	2.40
15.00	2.00	0.10	34.91	2.33
18.00	2.00	0.10	42.13	2.34
21.50	2.00	0.10	50.96	2.43
24.00	2.00	0.10	60.98	2.54
12.00	2.00	0.04	38.88	3.24
12.00	2.00	0.06	33.39	2.78
12.00	2.00	0.08	31.48	2.62
12.00	2.00	0.10	28.95	2.41
12.00	2.00	0.12	27.48	2.29
12.00	2.00	0.14	26.39	2.20
12.00	2.00	0.16	23.56	1.96
12.00	2.00	0.18	21.42	1.78
12.00	1.00	0.10	46.81	3.90
12.00	2.00	0.10	28.86	2.40
12.00	3.00	0.10	25.86	2.16
12.00	4.00	0.10	19.80	1.65
12.00	5.00	0.10	15.94	1.33
12.00	6.00	0.10	14.33	1.19
12.00	7.00	0.10	13.40	1.12
12.00	8.00	0.10	12.01	1.00
12.00	9.00	0.10	11.06	0.92

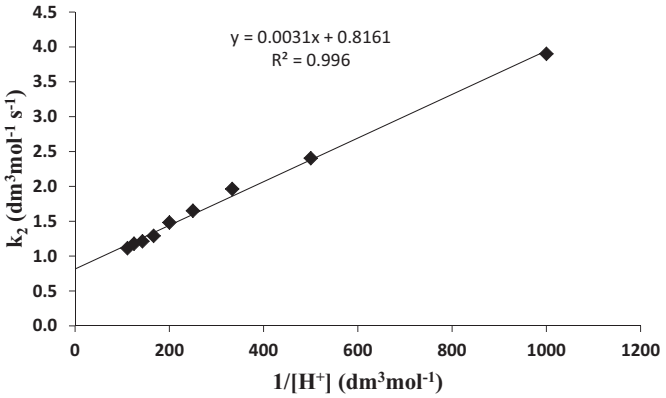

Figure 4. Graph of k_2 against $1/[H^+]$ for reaction of $[Co(Salophen)]^+$ and H_2A reaction at $[Co(Salophen)^+] = 3.0 \times 10^{-4}$ mol dm^{-3}, $[H_2A] = 12.0 \times 10^{-3}$ mol dm^{-3}, $[H^+] = (1.0–9.0) \times 10^{-3}$ mol dm^{-3}, $\mu = 0.1$ mol dm^{-3}, T = 33 ± 1°C, $\lambda_{max} = 470$ nm.

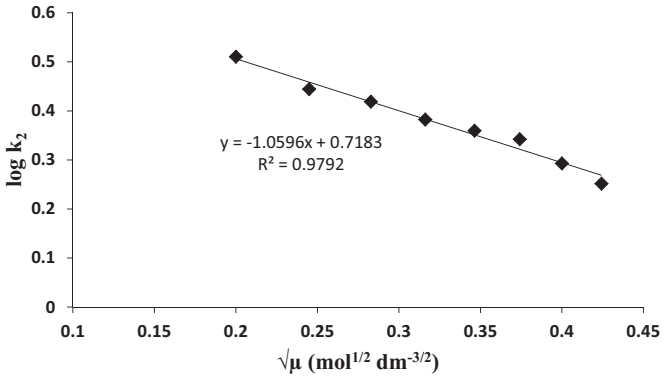

Figure 5. Graph of log k_2 versus $\sqrt{\mu}$ for the reaction of $[CoSalophen]^+$ and LSH at $[CoSalophen^+] = 3.0 \times 10^{-4}$ mol dm^{-3}, $[H_2A] = 12.0 \times 10^{-3}$ mol dm^{-3}, $[H^+] = 2.0 \times 10^{-3}$ mol dm^{-3}, $\mu = (0.04–0.18)$ mol dm^{-3}, T = 33 ± 1°C, and $\lambda_{max} = 470$ nm.

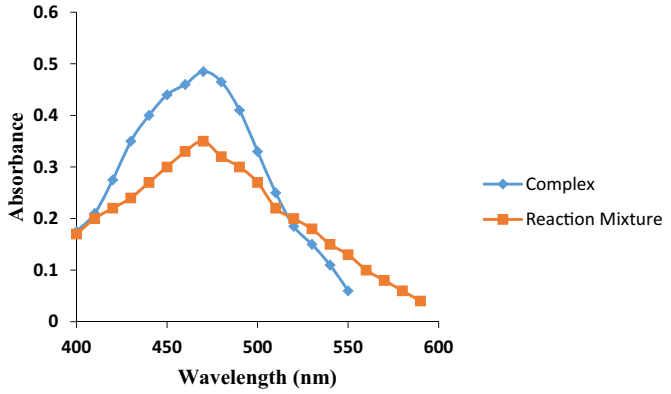

Figure 6. Plot for spectrophotometric test for the reaction of $[Co(Salophen)]^+$ and H_2A at $[Co(Salophen)^+] = 3.0 \times 10^{-4}$ mol dm^{-3}, $[H_2A] = 12.0 \times 10^{-3}$ mol dm^{-3}, $[H^+] = 2.0 \times 10^{-3}$ mol dm^{-3}, $\mu = 0.1$ mol dm^{-3}, T = 33 ± 1°C and $\lambda_{max} = 470$ nm.

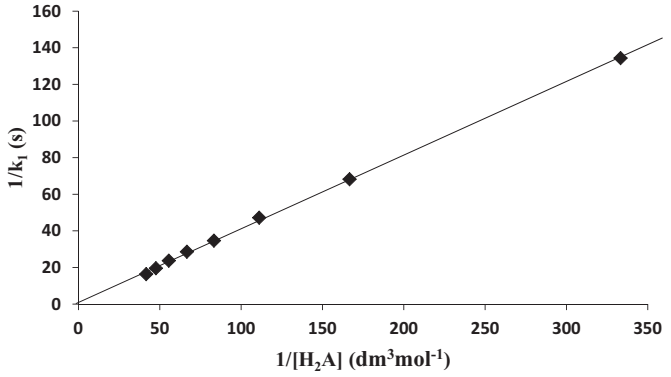

Figure 7. Michaelis-Menten plot for the reaction of $[Co(Salophen)]^+$ and H_2A at $[Co(Salophen)^+] = 3.0 \times 10^{-4}$ mol dm^{-3}, $[H_2A] = 12.0 \times 10^{-3}$ mol dm^{-3}, $[H^+] = 2.0 \times 10^{-3}$ mol dm^{-3}, $\mu = 0.1$ mol dm^{-3}, T = 33 ± 1°C, and $\lambda_{max} = 470$ nm.

Table 2. Added ions effect on the rate of reaction of $[Co(Salophen)]^+$ and H_2A at $[Co(Salophen)^+] = 3.0 \times 10^{-4}$ mol dm^{-3}, $[H_2A] = 12.0 \times 10^{-3}$ mol dm^{-3}, $[H^+] = 2.0 \times 10^{-3}$ mol dm^{-3}, $\mu = 0.1$ mol dm^{-3}, T = 33 ± 1°C and $\lambda_{max} = 470$ nm.

[X]	10^3 [X] (mol dm^{-3})	10^2 k_1 (s^{-1})	k_2 (dm^3 mol^{-1}s^{-1})
SO_4^{2-}	0.0	2.89	2.40
	3.0	3.10	2.58
	6.0	3.38	2.82
	9.0	3.62	3.01
	12.0	3.87	3.22
	15.0	4.09	3.41
	18.0	4.35	3.62
Mg^{2+}	0.0	2.89	2.40
	3.0	3.07	2.56
	6.0	3.19	2.66
	9.0	3.65	3.04
	12.0	3.74	3.11
	15.0	4.41	3.67
	18.0	4.98	4.15

Table 3. Temperature dependent rate constants and activation parameters for the reaction of $[Co(Salophen)]^+$ and H_2A at $[Co(Salophen)^+] = 3.0 \times 10^{-4}$ mol dm^{-3}, $[H_2A] = 12.0 \times 10^{-3}$ mol dm^{-3}, $[H^+] = 2.0 \times 10^{-3}$ mol dm^{-3}, $\mu = 0.1$ mol dm^{-3}, T = 33 ± 1°C, and $\lambda_{max} = 470$ nm.

T, K	10^2 k_1 (s^{-1})	k_2 (dm^{3}mol^{-1}s^{-1})
306	2.89	2.40
311	2.95	2.46
317	5.41	4.51
322	5.67	4.72
327	8.84	7.37
333	12.03	10.03
Activation Parameters		
$\Delta H^{\ddagger}$ = +47.70 kJ mol^{-1} $\Delta S^{\ddagger}$ = -82.87 J mol^{-1} K^{-1}		
$\Delta G^{\ddagger}$ = +73.06 kJ mol^{-1} at 300K E_a = +50.24 kJ mol^{-1}		

$$\text{Rate} = \frac{Kk_3[Co(Salophen)^+][H_2A]}{[H^+]} + k_4[Co(Salophen)^+][H_2A] \quad (13)$$

$$\text{Also, Rate} = k^1\,([Co(Salophen)^+]\,[H_2A]) \quad (14)$$

where $k^1 = k_3 + Kk_4\,[H^+]^{-1}$

Eq. (14) is similar to the experimental rate law (Eq. (4)).

4. Conclusion

The kinetic study and mechanism of the reaction between $[Co(Salophen)^+]$ and H_2A in a DMSO-Water medium (DMSO: H_2O; 1:4) revealed a 2:3 stoichiometry. The reaction is 1st order in both reactants which gives second-order overall. The rate of the reaction revealed two

pathways and also showed a negative effect of Brønsted–Debye salt. Kinetic and spectroscopic studies revealed no proof for the formation of an intermediate complex of significant stability during the reaction. Due to these outcomes, an outer sphere mechanism was proposed as the plausible pathway for the reaction.

Declarations

Author contribution statement

Safiya Abdulsalam: Performed the experiments; Analyzed and interpreted the data; Wrote the paper.

Sulaiman O. Idris: Conceived and designed the experiments.

Gideon A. Shallangwa, Ameh D. Onu: Contributed reagents, materials, analysis tools or data.

Funding statement

This research did not receive any specific grant from funding agencies in the public, commercial, or not-for-profit sectors.

Competing interest statement

The authors declare no conflict of interest.

Additional information

No additional information is available for this paper.

Acknowledgements

The authors would like to use this medium to express our sincere gratitude to all the staff and research teams of the Department of Chemistry, Ahmadu Bello University Zaria, Nigeria.

References

Abdulsalam, S., Idris, S.O., Shallangwa, G.A., Onu, A.D., 2020. Reaction of N, N^1-phenylenebis(salicylideneiminato)cobalt(III) and l-cysteine in mixed aqueous medium: kinetics and mechanism. Heliyon.

Abiti, B.Y., Onu, A.D., Idris, S.O., Ahmed, Y., Ilyasu, S.S., 2018. Kinetics and mechanism of the catalysed reduction of ethylenediaminetetraacetatocobaltate (III) ion by l-ascorbic acid in aqueous acidic medium. FUW Trends Sci. Tech. J. 3 (2B), 832–837.

Alioke, C.U., Ukoha, P.O., Ukwueze, N.N., Ujam, O.T., Asegbeloyin, J.N., 2012. Kinetics and mechanism of the reduction of N, N'-salicylideneiminationiron (III) complex ion by L-ascorbic acid in aqueous acid medium. Chem. Mater. Res. 2 (7), 48–57.

Blazevic, A., Hummer, A.A., Heffeter, P., Berger, W., Filipits, M., Cibin, G., Keppler, B.K., Rompel, A., 2017. Electronic state of sodium trans-[Tetrachloridobis (1H-indazole) ruthenate (III)](NKP-1339) in tumor, liver and kidney tissue of a SW480-bearing mouse. Sci. Rep. 7, 40966.

Bonnitcha, P.D., Kim, B.J., Hocking, R.K., Clegg, J.K., Turner, P., Neville, S.M., Hambley, T.W., 2012. Cobalt complexes with tripodal ligands: implications for the design of drug chaperones. Dalton Trans. 41 (37), 11293–11304.

Chiang, L., Allan, L.E.N., Alcantara, J., Wang, M.C.P., Storr, T., Shaver, M.P., 2014. Tuning ligand electronics and peripheral substitution on cobalt salen complexes: structure and polymerisation activity. Dalton Trans. 43 (11), 4295–4304.

Chiang, L., Kochem, A., Jarjayes, O., Dunn, T.J., Vezin, H., Sakaguchi, M., Ogura, T., Orio, M., Shimazaki, Y., Thomas, F., 2012. Radical localization in a series of symmetric NiII complexes with oxidized salen ligands. Chem. Eur. J. 18 (44), 14117–14127.

Clarke, R.M., Storr, T., 2016. Tuning electronic structure to control manganese nitride activation. J. Am. Chem. Soc. 138 (47), 15299–15302.

Davies, M.B., 1992. Reactions of L-ascorbic acid with transition metal complexes. Polyhedron 11 (3), 285–321.

Denny, W.A., 2010. Hypoxia-activated prodrugs in cancer therapy: progress to the clinic. Future Oncol. 6 (3), 419–428.

Dixon, D.A., Sadler, N.P., Dasgupta, T.P., 1995. Mechanism of the oxidation of L-ascorbic acid by the pentaammineaquacobalt (III) ion in aqueous solution. Transit. Met. Chem. 20 (3), 295–299.

Failes, T.W., Cullinane, C., Diakos, C.I., Yamamoto, N., Lyons, J.G., Hambley, T.W., 2007. Studies of a cobalt (III) complex of the MMP inhibitor marimastat: a potential hypoxia-activated prodrug. Chem. Eur. J. 13 (10), 2974–2982.

Graf, N., Lippard, S.J., 2012. Redox activation of metal-based prodrugs as a strategy for drug delivery. Adv. Drug Deliv. Rev. 64 (11), 993–1004.

Gupta, K.S., Gupta, Y.K., 1984. Hydrogen-ion dependence of reaction rates and mechanism. American Chemical Society Publications J. Chem. Edu. 61 (11), 972–977.

Gust, R., Ott, I., Posselt, D., Sommer, K., 2004. Development of cobalt (3, 4-diarylsalen) complexes as tumor therapeutics. J. Med. Chem. 47 (24), 5837–5846.

Ibrahim, I., Idris, S.O., Abdulkadir, I., Onu, A.D., 2019a. Kinetics and mechanism of the redox reaction of N, N′-phenylenebis-(salicylideneiminato) iron (III) with oxalic acid in mixed aqueous medium. Transit. Met. Chem. 44 (3), 269–273.

Ibrahim, I., Idris, S.O., Abdulkadir, I., Onu, A.D., 2019b. Redox reaction of N, N′-phenylenebis-(salicylideneiminato) iron (III) by hypophosphorus acid in mixed aqueous medium. Transit. Met. Chem.

Idris, S.O., Suleman, J.O., Iyun, J.F., Osunlaja, A.A., 2015. Reduction of 3, 7-bis (dimethylamino) phenazothionium chloride by benzenethiol in aqueous nitric acid medium: a mechanistic approach. J. Am. Chem. Soc. 5 (4), 313–321.

Jattinagoudar, L.N., Byadagi, K.S., Shirhatti, N.M., Nandibewoor, S.T., Chimatadar, S.A., 2013. Oxidation of ascorbic acid by hexacyanoferrate(III) in aqueous perchloric acid medium-A kinetic and mechanistic study. J. Chem. Pharmaceut. Res. 5 (4), 290–300.

Jena, P., Priyambada, J., Acharya, A.N., Acharya, A.N., Mundlapati, V.R.A.O., Mundlapati, V.R.A.O., Dash, A.C., Dash, A.C., Biswal, H.S., Biswal, H.S., 2018. Kinetics and mechanistic study of the reduction of Mn III by oxalate in Salophen scaffold: relevance to oxalate oxidase. J. Chem. Sci. 130 (9), 123.

Khan, M.M.T., Shukla, R.S., 1988. Inner sphere oxidation of L-ascorbic acid by Ru (III) ion and its complexes in aqueous acidic medium. Inorg. Chim. Acta. 149 (1), 89–94.

Kianfar, A.H., Khavasi, H.R., 2016. Synthesis and crystal structure of cobalt (III) complexes of salen type schiff bases and tertiary phosphanes as ligands. Inorganic Chem. Res. 1 (2), 105–114.

Kizaka-Kondoh, S., Inoue, M., Harada, H., Hiraoka, M., 2003. Tumor hypoxia: a target for selective cancer therapy. Canc. Sci. 94 (12), 1021–1028.

Liou, Y.W., Wang, C.M., 2000. Peroxidase mimicking: Fe (Salen) Cl modified electrodes, fundamental properties and applications for biosensing. Elsevier J. Electroanal. Chem. 481 (1), 102–109.

Lippert, B., 1999. Cisplatin: Chemistry and Biochemistry of a Leading Anticancer Drug. John Wiley & Sons.

Mari, C., Pierroz, V., Ferrari, S., Gasser, G., 2015. Combination of Ru (II) complexes and light: new frontiers in cancer therapy. Chem. Sci. 6 (5), 2660–2686.

Onu, A.D., Iyun, J.F., Idris, S.O., 2009. The kinetics of the reduction of tetraoxoiodate (VII) by n-(2-hydroxylethyl) ethylenediaminetriacetatocobaltate (II) ion in aqueous perchloric acid. J. Trans. Metal Chem. 34 (8), 849–853.

Osunlaja, A.A., Idris, S.O., Iyun, J.F., 2013. Kinetics and mechanism of thiourea oxidation by oxygenated $[Co_2(O_2)(NH_3)_{10}]^{5+}$ complex. J. Chem. Pharmaceut. Res. 5 (2), 328–336.

Pizarro, A.M., Habtemariam, A., Sadler, P.J., 2010. Activation mechanisms for organometallic anticancer complexes. In: Medicinal Organometallic Chemistry. Springer, pp. 21–56.

Pizzolato, E., Natali, M., Posocco, B., López, A.M., Bazzan, I., Di Valentin, M., Galloni, P., Conte, V., Bonchio, M., Scandola, F., 2013. Light driven water oxidation by a single site cobalt salophen catalyst. Chem. Commun. 49 (85), 9941–9943.

Renfrew, A.K., 2014. Transition metal complexes with bioactive ligands: mechanisms for selective ligand release and applications for drug delivery. Metallomics 6 (8), 1324–1335.

Renfrew, A.K., Bryce, N.S., Hambley, T.W., 2013. Delivery and release of curcumin by a hypoxia-activated cobalt chaperone: a XANES and FLIM study. Chem. Sci. 4 (9), 3731–3739.

Salavati-niasari, M., 2006. Host (nanocavity of zeolite-Y)– guest (tetraaza [14] annulene copper (II) complexes) nanocomposite materials: synthesis, characterization and liquid phase oxidation of benzyl alcohol, 245, pp. 192–199.

Salem, I.A., Gemeay, A.H., 1996. Kinetics and mechanism of the oxidation of L-ascorbic acid by the N, N′-ethylenebis (salicylideneiminato) manganese (III) complex in aqueous solution. Transit. Met. Chem. 21 (2), 130–134.

Subramaniam, P., Vanitha, T., Kodispathi, T., Sundari, S., Raj, C., 2014. Role of iron (III)-salen chloride as oxidizing agent with thiodiglycolic acid: the effect of axial ligands. J. Mexican Chem. Soc. 58 (2), 211–217.

Ukoha, P.O., Anidobu, C.O., Iorungwa, P.D., Oluigbo, I.C., 2018. Kinetics and mechanism of reduction of $[(Fe\ (saloph))_2$-μ-dicarpy] complex by l-ascorbic acid in acid medium. FUW Trends Sci. Technol. J. 3 (1), 158–162.

Ware, D.C., Palmer, H.R., Brothers, P.J., Rickard, C.E.F., Wilson, W.R., Denny, W.A., 1997. Bis-tropolonato derivatives of cobalt (III) complexes of bidentate aliphatic nitrogen mustards as potential hypoxia-selective cytotoxins. J. Inorg. Biochem. 68 (3), 215–224.

Webb, M.I., Walsby, C.J., 2013. EPR as a probe of the intracellular speciation of ruthenium (III) anticancer compounds. Metallomics 5 (12), 1624–1633.

Yamamoto, N., Renfrew, A.K., Kim, B.J., Bryce, N.S., Hambley, T.W., 2012. Dual targeting of hypoxic and acidic tumor environments with a cobalt (III) chaperone complex. J. Med. Chem. 55 (24), 11013–11021.

Yilmaz, H., Kocak, A., Dilimulati, M., Zorlu, Y., Andac, M., 2017. A new Co (III) complex of Schiff base derivative for electrochemical recognition of nitrite anion. J. Chem. Sci. 129 (10), 1559–1569.

Zhang, C., Sutherland, M., Herasymchuk, K., Clarke, R.M., Thompson, J.R., Chiang, L., Walsby, C.J., Storr, T., 2017. Octahedral Co (III) salen complexes: the role of peripheral ligand electronics on axial ligand release upon reduction. Can. J. Chem. 96 (2), 110–118.